ELSEVIER

www.elsevier.nl/locate/jorganchem

Journal of Organometallic Chemistry 603 (2000) 69–79

Journal of Organometallic Chemistry

Chiral molybdenum(VI) and tungsten(VI) 2′-pyridinyl alcoholate complexes. Synthesis, structure and catalytic properties in asymmetric olefin epoxidation

Wolfgang A. Herrmann *, Joachim J. Haider [1], Jörg Fridgen, Gerhard M. Lobmaier [2], Michael Spiegler

Anorganisch-chemisches Institut der Technischen Universität München, Lichtenbergstr. 4, D-85747 Garching, Germany

Received 15 November 1999

Abstract

A new class of chiral molybdenum(VI) and tungsten(VI) complexes of the type $MO_2L^*_2$ (M = Mo, W; L* = chiral 2′-pyridinyl alcoholate), available through several synthetic pathways, and their catalytic behavior in the asymmetric epoxidation of unfunctionalized olefins are reported. MO_2Cl_2, $MO_2(acac)_2$, and $Na_2[MO_4]$ (M = Mo, W) served as starting materials for the synthesis of the chiral molybdenum(VI) or tungsten(VI) complexes, respectively. The new oxo complexes were fully characterized including X-ray crystallographic analyses. The chiral 2′-pyridinyl alcoholate ligands were derived from either (−)-menthone, (−)-fenchone, (−)-camphor or (+)-camphor. For catalytic runs in the enantioselective epoxidation, *trans*-methylstyrene was used as model substrate and *tert*-butylhydroperoxide as the oxidant. The molybdenum complexes exhibit good catalytic activity and substantial optical induction. By way of contrast, the analogous tungsten complexes have low activities at comparable optical yields.

Keywords: Molybdenum; Tungsten; Asymmetric catalysis; Epoxidation; 2′-Pyridinyl alcoholate

1. Introduction

Recently, we described the synthesis of new dioxomolybdenum(VI) complexes of the type $Mo_2O_2L_2$ (L = 2′-pyridinyl alcoholate) and their application as catalysts for the selective oxidation of terminal *n*-alkenes with molecular oxygen and hydroperoxides [1,2]. We also reported the analogous dioxotungsten(VI) complexes [3]. Other ligand systems [4] are known for olefin epoxidation but the use of 2′-pyridinyl alcoholate ligands is attractive because they can be easily prepared in a broad range by the reaction of 2-lithiopyridine with symmetric ketones. This has already been successfully demonstrated for various 2′-pyridinyl alcoholates bearing aryl or alkyl moieties, respectively (Fig. 1) [5].

The important feature of these ligands is their strong resistance to ligand degradation which is crucial for the application in oxidation catalysis [6]. In our case this

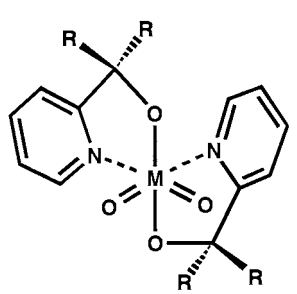

Alkyl: R = H, CH_3, C_2H_5, $CH(CH_3)_2$

Aryl: R = C_6H_5, $C_6H_4{}^tBu$, $C_6H_4OCH_3$, C_6H_4I

Fig. 1. Structure of achiral molybdenum(VI) and tungsten(VI) 2′-pyridinyl alcoholate complexes.

* Corresponding author. Tel.: +49-89-32093080; fax: +49-89-28913473.

E-mail address: lit@arthur.anorg.chemie.tu-muenchen.de (W.A. Herrmann)

[1] Present address: Bayer AG, KA-F + E/KCH, F41, D-4153g Dormagen, Germany.

[2] Present address: Grünau-Illertissen GmbH, Postfach 1063, D-89251 Illertissen, Germany.

0022-328X/00/$ - see front matter
PII: S0022-328X(00)00112-1

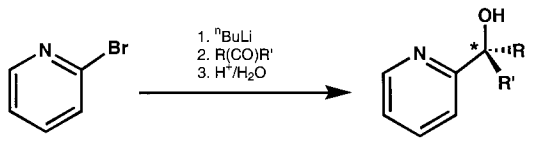

Scheme 1. Diastereoselective synthesis of chiral 2′-pyridinyl alcohols using ketones from the chiral pool.

has been achieved by the use of tertiary alcohol and pyridine as oxidation-stable functional groups.

If unsymmetrical ketones are used as starting material for ligand synthesis chiral 2′-pyridinyl alcoholates are obtained [7]. For this reason we also became interested in the evaluation of our ligand concept for catalytic asymmetric applications. In the field of molybdenum chemistry several approaches for catalytic asymmetric epoxidation have been reported but none have yielded high enantiomeric excess [4]. The catalytically active species is normally prepared in situ from $MoO_2(acac)_2$, *tert*-butylhydroperoxide and an excess of chiral *N*/*O* or *O*/*O*-ligands, e.g. *N*-alkyl ephedrine [4a], *N*-methylprolinol [4b] or diisopropyl tartrate [4d]. In the case of *N*-methylprolinol the secondary alcohol at the single chiral center is presumably subject to oxidation which erases the chirality in the ligand [4b]. This detrimental effect can be eliminated in the case of chiral 2′-pyridinyl alcohols. For this reason we have expanded our studies of this synthetic strategy to chiral 2′-pyridinyl alcohols by using a straightforward approach that leads directly to stereoisomerically pure materials in one step. Early results proved our strategy both in ligand and complex synthesis and in asymmetric epoxidation catalysis [8]. We now report the synthesis and characterization of chiral complexes of the type $MO_2L^*_2$ (M = Mo, W; L* = chiral 2′-pyridinyl alcoholate) and describe the evaluation of their catalytic potential in the asymmetric epoxidation of unfunctionalized olefins.

2. Results and discussion

2.1. Diastereoselective synthesis of chiral 2′-pyridinyl alcohols

There are two synthetic pathways for the synthesis of enantiomerically pure 2′-pyridinyl alcohols. One strategy involves the formation of a racemic mixture of 2′-pyridinyl alcohols from the addition of 2-lithiopyridine to unsymmetrical ketones followed by kinetic resolution of the enantiomers. This can be achieved by acylation of the alcohol, enzymatic cleavage of one enantiomer and subsequent chromatographic separation [9]. The other method uses the synthesis of α-ketopyridines from 2-lithiopyridine and appropriate nitriles followed by reductive hydrogenation to a single enantiomer of the chiral 2′-pyridinyl alcohol employing chiral reducing agents such as chlorodiisopinocampheylborane [10]. We decided to investigate the reaction of 2-lithiopyridine with appropriate prochiral ketones from the chiral pool [7] which directly leads to diastereomerically pure 2′-pyridinyl alcohols as convenient alternative.

As it can be clearly seen from Scheme 1, the nucleophilic attack of 2-lithiopyridine at carbonyl groups is always preferred from the sterically less hindered side which corresponds to the predicted attack according to the model of Felkin and Ahn [11].

Due to the constraint of the molecular geometry in the norbornane backbone or bulky side chains such as an isopropyl group, (+)-camphor (**1**), (−)-fenchone (**2**) and (−)-menthone (**3**) are high-rated candidates for this synthetic strategy (Fig. 2).

The carbonyl groups in camphor and fenchone are accessible from different stereosides. Camphor is obviously attacked from the *endo*-side due to the sterically demanding methyl group at the C1-bridge of the norbornane backbone whereas the nucleophilic addition to fenchone is exclusively performed from the *exo*-side. Since in fenchone two geminal methyl groups are located in α-position to the carbonyl group, the addition of 2-lithiopyridine is guided by the higher steric demand of the C2 bridge compared to the C1-bridge.

The reaction products, i.e. the desired ligands, (1*R*,2*R*,4*R*) - 1,7,7 - trimethyl - 2 - (2′ - pyridinyl)bicyclo-[2.2.1]heptan-2-ol (**4**) ((+)-campy), (1*S*,2*S*,4*S*)-1,7,7-trimethyl-2-(2′-pyridinyl)bicyclo-[2.2.1]heptan-2-ol (**5**) ((−)-campy), (1*R*,2*R*,4*S*)-1,3,3-trimethyl-2-(2′-pyridinyl)bicyclo[2.2.1]heptan-2-ol (**6**) ((−)-fenpy) (1*S*,2*S*,5*R*)-5-methyl-2-isopropyl-1-(2′-pyridinyl)cyclohexan-1-ol (**7**) ((−)-menpy), shown in Fig. 2, were prepared and were fully characterized. The ^{1}H-NMR signals were completely assigned by 2D-NMR techniques and X-ray crystallography was used to confirm the absolute configuration of the ligand (cf. (−)-fenpy (**6**) in Fig. 3) (Tables 1 and 2).

2.2. Synthesis of chiral dioxomolybdenum(VI) and dioxotungsten(VI) complexes

For the development of a straightforward synthetic route to dioxomolybdenum(VI) and dioxotungsten(VI) 2′-pyridinyl alcoholate complexes **13**–**20**, three different metal precursors bearing the *cis*-dioxo metal fragment were tested (Scheme 2).

Starting with the dioxodichlorides MoO_2Cl_2 (**7**) or WO_2Cl_2 (**8**) we found that, despite its poor solubility in organic solvents, WO_2Cl_2 (**8**) reacts with 2′-pyridinyl alcohols in refluxing THF where a THF-adduct is presumably formed as intermediate. Both chloro ligands are replaced by the pyridinyl alcohols to form complexes of the type WO_2L_2 (L = 2′-pyridinyl alcoholate) (**17**–**20**). The products are obtained as microcrystalline colorless air- and moisture-resistant solids. In the

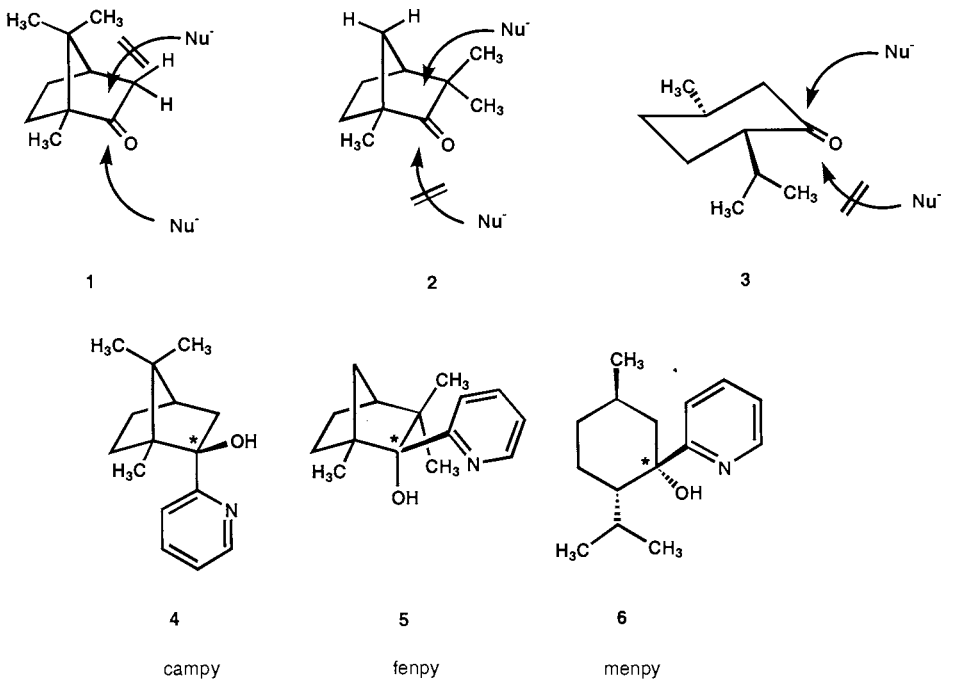

Fig. 2. Examples for chiral 2′-pyridinyl alcohols as ligands.

case of MoO_2Cl_2 (**7**) the molybdenum–chlorine bond is not cleaved by our ligands. If, however, the 2′-pyridinyl alcohol is deprotonated with *n*-butyllithium, the lithium alcoholate reacts with MoO_2Cl_2 (**7**) and the desired MoO_2L_2 complexes **13**–**16** (L = 2′-pyridinyl alcoholate) are formed.

In an alternative approach we also demonstrated the suitability of dioxobis(acetylacetonato) compounds $MoO_2(acac)_2$ (**9**) and $WO_2(acac)_2$ (**10**), respectively, as versatile precursors for ligand substitution. They are much easier to handle than the dioxodichlorides because of their high resistance to air and moisture. The dioxobis(acetylacetonato) compounds react with two equivalents of 2′-pyridinyl alcohol in dry methanol to form the pyridinyl alcoholate complexes (**13**)–(**20**) of analytical purity in high yields. Depending upon the substituents at the quaternary α-carbon of the 2′-pyridinyl alcohol, the complexes either precipitate immediately or after partial removal of the solvent. In our case the chiral ligands bear bulky hydrophobic hydrocarbon substituents. Therefore the complexes precipitate immediately after addition of the ligand to a methanol solution of the respective dioxobis(acetylacetonato) compound and can be filtered off.

Finally, we found a way to use the metal salts $Na_2[MoO_4]$ (**11**) and $Na_2[WO_4]$ (**12**) as the most inexpensive and easy-to-handle starting materials to prepare the aforesaid type of 2′-pyridinyl alcoholate complexes. A solution of the corresponding ligand in acetic acid is

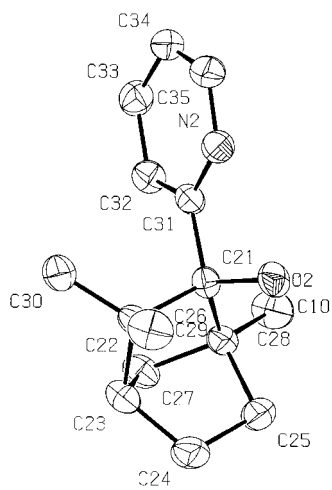

Fig. 3. PLATON-representation of (1*R*,2*S*,4*S*)-1,3,3-trimethyl-2-(2′-pyridinyl)bicyclo[2.2.1]-heptan-2-ol (−)-fenpy (**6**). Thermal ellipsoids represent 50% probability levels.

Table 1
Selected bond lengths (pm) and bond angles (°) of (−)-fenpy (**6**)

Bond lengths		Bond angles	
C11–N1	134.0(3)	C11–N1–C15	119.2(19)
C15–N1	133.3(3)	N1–C11–C1	113.7(17)
C11–C1	154.0(3)	C11–C1–O1	106.8(15)
O1–H	91.0(3)	O1–C1–C2	112.4(16)
C1–O1	142.7(2)	O1–C1–C6	107.6(15)
		N1–C11–C12	120.8(19)

Table 2
Crystallographic data and measuring parameters for (−)-fenpy (**6**)

Compound	(−)-fenpy (**6**)
M_r	231.34 ($C_{15}H_{21}NO$)
Crystal system	Monoclinic
a (pm)	2547.95(19)
b (pm)	753.29(3)
c (pm)	1368.79(10)
β (°)	100.212(4)
V (10^6 pm^3)	2585.6(3)
Space group (no.)	$C2$ (5)
D_{calc}	1.189
l (pm)	154.178 (Cu–K_α)
Z	8
F (000)	1008
μ (cm^{-1})	5.7
hkl-Range	−30/30, −9/9, −16/0
θ Range (°)	3.8–67.8
T (K)	193
No. of reflections measured	4739
No. of unique reflections	4535
No. of used reflections ($I/\sigma(I)>0.001$)	4535
No. of parameters	475
Residual electron density (e Å^{-3})	0.24/−0.29
Flack parameter	−0.2(2)
[a] R_1	0.0535
[a] wR_2	0.1135
GoF [a]	1.085

[a] $R_1 = \Sigma(||F_o|-|F_c||)/\Sigma|F_o|$, $wR_2 = [\Sigma w(|F_o|-|F_c|)^2/\Sigma wF_o^2]^{1/2}$.

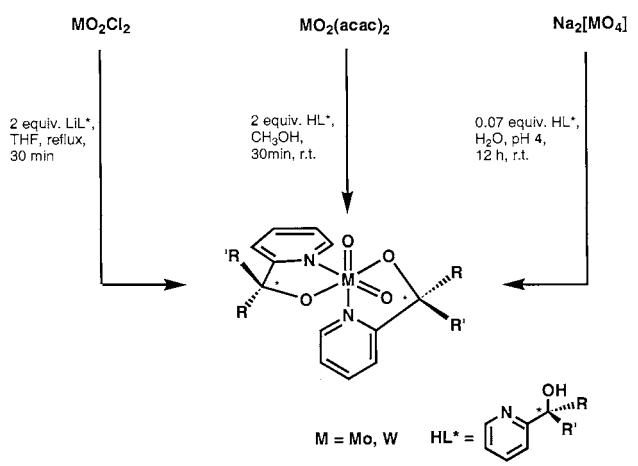

Scheme 2. Synthetic pathways to complexes of the type $MO_2L_2^*$ (M = Mo, W) using different oxometal precursors.

added to an excess of the respective metal salt in aqueous solution. The solution turns turbid and after stirring overnight the product can be filtered off. Compared to the previous approaches this method is favorable both for economic and ecological reasons, since inexpensive starting materials and environmentally benign solvent, water, are employed. It also successfully demonstrates the excellent stability of the dioxomolybdenum(VI) and tungsten(VI) 2′-pyridinyl alcoholate complexes towards moisture.

All molydenum and tungsten complexes of the type $MO_2L_2^*$ (M = Mo, W) derived from the four chiral ligands were prepared and fully characterized. In the complexes **13**–**20**, an approximately 15 ppm downfield shift of the quaternary alcoholate carbon atom signal in the ^{13}C-NMR spectrum indicates the coordination to the metal center. Another NMR probe is represented by the C2′ carbon atom in ortho position to the nitrogen atom at the pyridine moiety (Table 3).

The infrared spectra show the typical symmetric and asymmetric M=O stretch vibrations in the region of 896 and 934 cm^{-1} indicating the presence of the cisoid dioxometal moiety in the complexes. The data obtained from elemental analysis and mass spectroscopy confirm the predicted structure type. At this level of characterization, however, the exact arrangement of the ligands at the metal center is not fully determined. For this reason we recrystallized the products from CH_3OH/$CHCl_3$ yielding colorless crystals and X-ray crystallographic analyses were performed. ORTEP-style plots of **13** and **19** are depicted in Figs. 4 and 5 as examples for a molybdenum and tungsten complex (Tables 4–6).

In both complexes two anionic *N*,*O*-chelating ligands and two oxo ligands are bound to the metal adopting a distorted octahedral coordination geometry around the molybdenum or tungsten center, respectively. The distortion from the idealized octahedral geometry arising from the acute bite angle of the bidentate *N*,*O*-ligands varies from 70.8° for $WO_2((-)$-fenpy$)_2$ (**19**) to 71.5° for $MoO_2((+)$-campy$)_2$ (**13**). As in MoO_2(acac)$_2$ (**7**), and WO_2(acac)$_2$ (**8**), dioxomolybdenum(VI) or dioxotungsten(VI) 2′-pyridinyl alcoholate complexes, two oxygen ligands and the metal form a oxometal fragment with a *cis*-arrangement. With 104.93° (**13**) and 105.40° (**19**) the bond angles of the *cis*-dioxo fragment remain unchanged. The neutral *N*-donor ligand atoms of the pyridine ring are in a *trans*-position to the *cis*-dioxo-

Table 3
Comparison of selected ^{13}C-NMR signals as indicator for coordination of the chelating ligands at the molybdenum or tungsten center, respectively [a]

Compound	δ (C_{OH}) (ppm)	δ ($C_{2'ortho}$) (ppm)
$MoO_2((+)$-campy$)_2$ (**13**)	96.41 (82.64)	166.07 (162.30)
$MoO_2((-)$-campy$)_2$ (**14**)	96.14 (82.65)	166.44 (163.54)
$MoO_2((-)$-fenpy$)_2$ (**15**)	99.62 (83.62)	164.94 (163.25)
$MoO_2((-)$-menpy$)_2$ (**16**)	92.82 (77.17)	169.65 (165.25)
$WO_2((+)$-campy$)_2$ (**17**)	94.81 (82.64)	166.06 (162.30)
$WO_2((-)$-campy$)_2$ (**18**)	95.83 (82.65)	167.06 (163.54)
$WO_2((-)$-fenpy$)_2$ (**19**)	99.42 (83.62)	165.57 (163.25)
$WO_2((-)$-menpy$)_2$ (**20**)	92.62 (77.17)	170.18 (165.35)

[a] NMR signals of the free ligand are given in brackets.

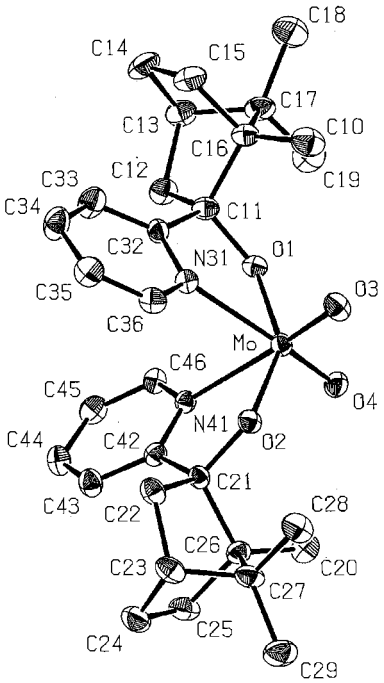

Fig. 4. PLATON-representation of $MoO_2((+)\text{-campy})_2$ (**13**). Thermal ellipsoids represent 50% probability levels.

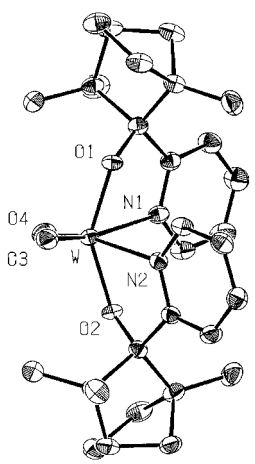

Fig. 5. PLATON-representation of $WO_2((-)\text{-fenpy})_2$ (**19**). Thermal ellipsoids represent 50% probability levels.

molybdenum fragment resulting from the *trans*-directing effect of the oxo ligands. The chelating ligands can bind in two different ways to the metal center forming a Δ- or Λ-isomer. Since we employed stereoisomerically pure ligands both isomers can be distinguished as diastereomers. In all cases we found only one set of signals in the ^{13}C-NMR spectrum. This means only one isomer is actually formed. A comparison of the crystal structures from a set of six complexes [12,13] demonstrates that molybdenum and tungsten complexes derived from (+)-campy and (−)-menpy prefer the Λ-form whereas the (−)-campy and (−)-fenpy-derived complexes favor the Δ-form.

2.3. Catalytic results

We examined the complexes described above for their activity in the asymmetric epoxidation of unfunctionalized olefins. This class of substrates is particularly interesting because the Jacobsen method works highly efficient only for *cis*-substituted olefins [14].

In the field of molybdenum-catalyzed asymmetric epoxidation, functionalized olefins, e.g. allylic alcohols or amides, are often chosen as substrates and yield enantiomeric excesses up to 53% [4b] whereas for unfunctionalized olefins only one procedure is known and that yields only a 14% e.e. [15] or only stoichiometric procedures are known [4c]. To the best of our knowledge, no asymmetric epoxidation procedure is known for tungsten-based systems [16].

For our catalytic experiments we chose *trans*-methylstyrene as model substrate and *tert*-butylhydroperoxide as oxidant (Scheme 3). In a typical catalytic run one equivalent of substrate was mixed with 1 mol% catalyst

Table 4
Selected bond lengths (pm) and bond angles (°) of $MoO_2((+)\text{-campy})_2$ (**13**)

Bond lengths		Bond angles	
Mo–O1(sb)	194.8(2)	O3–Mo–O4	105.4(11)
Mo–O2	194.4(2)	O2–Mo–O4	105.6(10)
Mo–O3(db)	170.6(2)	O1–Mo–N1	71.6(9)
Mo–O4	169.9(2)	O4–Mo–N2	71.4(10)
Mo–N1	233.9(2)	N1–Mo–N2	79.2(8)
Mo–N2	232.1(2)	O1–Mo–O2	147.5(12)
O1–C1	144.0(4)	Mo–N1–C11	114.5(18)
C1–C11	152.6(5)	N1–C11–C1	114.2(3)
C11–N1	133.9(4)	N2–C31–C21	113.3(3)
O2–C21	142.9(4)	C11–C1–O1	106.1(3)
C21–C31	153.0(4)	C31–C21–O2	106.9(2)
C31–N2	134.7(4)	C1–O1–Mo	129.7(3)
		C21–O2–Mo	130.0(18)

Table 5
Selected bond lengths (pm) and bond angles (°) of $WO_2((-)\text{-fenpy})_2$ (**19**)

Bond lengths		Bond angles	
W–O1 (sb)	193.1(19)	O1–W–O2	146.7(9)
W–O2	193.4(18)	O1–W–O3	93.4(9)
W–O3 (db)	173.4(2)	O3–W–N1	70.8(8)
W–O4	173.9(2)	O4–W–N2	71.4(10)
W–N1	232.5(2)	N1–W–N2	86.9(8)
W–N2	232.1(2)	O3–W–O4	104.9(10)
O1–C1	142.2(3)	W–N1–C11	115.3(18)
C1–C11	153.7(4)	N1–C11–C1	113.7(2)
C11–N1	134.0(3)	N2–C31–C21	113.9(2)
O2–C21	142.2(3)	C11–C1–O1	106.0(2)
C21–C31	153.1(4)	C31–C21–O2	106.0(2)
C31–N2	134.2(3)	C1–O1–W	128.8(15)
		C21–O2–W	128.5(15)

Table 6
Crystallographic data and measuring parameters for $MoO_2((+)$-campy)$_2$ (**13**) and $WO_2((-)$-fenpy)$_2$ (**19**)

Compound	$MoO_2((+)$-campy)$_2$ (**13**)	$WO_2((-)$fenpy)$_2\cdot CH_3OH$ (**19**)
Empirical formula	$C_{30}H_{40}N_2O_4Mo$	$C_{31}H_{44}N_2O_5W$
M_r	588.60	740.58
Crystal system	Monoclinic	Orthorhombic
a (pm)	1355.38(7)	1389.37(2)
b (pm)	831.79(2)	1481.01(2)
c (pm)	1381.79(7)	1529.73(2)
β (°)	116.880(5)	90
V (10^6 pm^3)	1389.5(1)	3147.7(7)
Space group (no.)	$P2_1$ (4)	$P2_12_12_1$ (19)
D_{calc}	1.407	1.563
l (pm)	71.073 (Mo–K_α)	71.073 (Mo–K_α)
Z	2	4
F (000)	616	1504
μ (cm^{-1})	5.1	–
hkl-Range	−15/15, −9/9, −16/16	−17/17, −14/14, −19/19
θ Range (°)	2.8–24.6	4.1–26.4
T (K)	193	293
No. of reflections measured	17 015	5854
No. of unique reflections	4520	5854
No. of used reflections ($I/\sigma(I)>0.001$)	4520	5831
No. of parameters	362	530
Residual electron density (e Å^{-3})	0.35/−0.46	0.84/−0.79
Flack parameter	−0.04(3)	–
[a] R_1	0.0286	0.0157
[a] wR_2	0.0477	0.0416
GoF [a]	0.916	1.06

[a] $R_1 = \Sigma(||F_o|-|F_c||)/\Sigma|F_o|$, $wR_2 = [\Sigma w(|F_o|-|F_c|)^2/\Sigma wF_o^2]^{1/2}$.

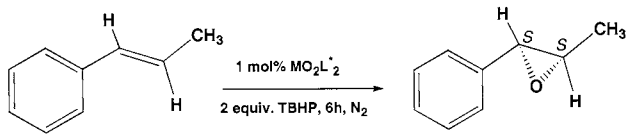

Scheme 3. Epoxidation of *trans*-methylstyrene (M = Mo, W).

and two equivalents of *tert*-butylhydroperoxide (S/C ratio 100) and the reaction was performed over 6 h at 50°C under exclusion of air and moisture. Aliquots were taken every 10 min and were quenched by addition of manganese dioxide and magnesium sulfate, filtered and analyzed by chiral gas chromatography. The results are depicted in Table 7.

A comparison of the catalytic activity reveals good conversions for all molybdenum complexes which are in the range of 70%. The tungsten complexes, however, were only half as active. The enantioselectivity, on the other hand, depends more strongly on the ligand than on the metal, e.g. complexes bearing the same ligand type gave similar results. The highest optical induction was 26% for the (*S*,*S*)-epoxide by using the (+)-campy-substituted complexes. When the (−)-campy substituted complexes were employed we observed the inversion of the optical induction with formation of the (*R*,*R*)-epoxide, as expected. This clearly shows the dependence of stereoselectivity on the enantiomeric nature of the ligand. When the chiral complexes are compared by terms of the influence of steric demand on the stereoselectivity, it can also be clearly seen that the bulkier norbornane-type ligands gave the highest optical inductions. These results are encouraging but also leave the question why the optical inductions for molybdenum and tungsten systems are poor compared to other systems [14]. Perhaps, this can be explained by detrimental effects from *tert*-butanol which is inevitably formed during the reaction from *tert*-butylhydroperoxide [17]. For example, the polarity of the solvent (toluene or methylene chloride) is increased by the formation of *tert*-butanol. Since for unfunctionalized olefins only non-covalent interactions between the catalytically-active species and the substrate can contribute to the optical induction, it is quite clear that polar solvent molecular would impair these interactions leading to lower enantiomeric excess. In a series of control experiments we employed several aliphatic alcohols, such as methanol, ethanol, isopropanol and *tert*-butanol, as the solvent. In all cases, no optical induction was observed although the system was still catalytically active. Another possible side effect of alcohols is their potential to function as additional monodentate ligands thus competing with the chelating ligand for the metal center. Since we prepared our system in a 100:200:1 ratio (substrate:oxidant:catalyst), it is also clear that a high excess of competitive achiral ligand is produced during the reaction.

This becomes more apparent when the reaction mechanism is considered. In a control experiment we prepared a stoichiometric mixture of a chiral molybdenum complex with *trans*-β-methylstyrene in the absence

Table 7
Comparison of the results for the molybdenum and tungsten-catalyzed asymmetric epoxidation of *trans*-β-methylstyrene [a]

Compound	Conversion (%)	e.e. (%)
$MoO_2((+)$-campy)$_2$ (**13**)	76	26
$MoO_2((-)$-campy)$_2$ (**14**)	73	25 [b]
$MoO_2((-)$-fenpy)$_2$ (**15**)	71	15
$MoO_2((-)$-menpy)$_2$ (**16**)	81	4
$WO_2((+)$-campy)$_2$ (**17**)	33	24
$WO_2((-)$-campy)$_2$ (**18**)	34	24 [b]
$WO_2((-)$-fenpy)$_2$ (**19**)	31	12
$WO_2((-)$-menpy)$_2$ (**20**)	36	4

[a] 1 mol% catalyst, two equivalents *tert*-butylhydroperoxide, 50°C, 6 h, N_2, molecular sieve (4 Å).

[b] By use of the enantiomeric (−)-campy ligand the (*R*,*R*)-epoxide was obtained.

of *tert*-butylhydroperoxide under nitrogen atmosphere. No reaction was observed which means that the oxo ligands of the *cis*-dioxomolybdenum fragment do not transfer oxygen to the olefin. An oxometal transfer mechanism under change of oxidation state at the molybdenum center, as found for the Jacobsen-type manganese salene complexes [14], can be clearly ruled out. Therefore, it is plausible to assume the existence of a peroxometal reaction pathway where the d^0 central metal acts as Lewis-acid to activate the hydroperoxide [18]. In our case since the molybdenum and tungsten centers are coordinatively saturated by an octahedral coordination sphere and the oxo ligands are 'chemically inert', the reaction mechanism therefore must involve a dissociative step with respect to the chelating ligand.

For this reason we prepared a stoichiometric mixture of an achiral dimethylsubstituted dioxomolybdenum(VI)-2′-pyridinyl alcoholate complex with *tert*-butylhydroperoxide and monitored the signals of the methyl groups in a temperature row by NMR. When the chelating ligand is bound to the metal center, the signal of the two methyl groups was split due to their different stereochemical environments. Only in the presence of an alkylhydroperoxide did the separate singlet bands collapse at about 60 °C indicating the existence of a dissociative step. Although the cleavage of a Mo–O or Mo–N bond cannot be distinguished in this experiment, it is plausible to assume that the Mo–O bond is cleaved with the subsequent addition of the hydroperoxide to the Lewis-acidic metal center. An 'oxenoid' oxygen is generated which is subsequently transferred to the olefin. The stereodifferentiation is then produced by the chiral centers through weak π–π-interactions between the pyridine ring of the ligand and the phenyl ring of the aromatic olefin. The catalytic tests in protic solvents yielded no optical induction at all to confirm this hypothesis.

3. Conclusion

Chiral 2′-pyridinyl alcoholates are suitable ligands for the application in catalytical asymmetric olefin epoxidation due to their high resistance to oxidative degradation. The ligands and their molybdenum(VI) and tungsten(VI) complexes can be obtained in good to excellent yields by a straightforward synthesis. The catalytic results show not only the suitability of this new system for asymmetric epoxidation but also some of the limitations when using *tert*-butylhydroperoxide as the oxidant. Efforts to identify more effective oxidants and catalysts for these reactions are being investigated in our laboratories.

4. Experimental

4.1. General remarks

All reactions were carried out under nitrogen with use of standard Schlenk techniques. Only freshly distilled, dry and oxygen-free solvents were used. The ^{1}H- and ^{13}C-NMR spectra were recorded at 399.65 and 100.53 MHz on a FT Jeol GX 400 instrument. IR spectra were recorded on a Perkin–Elmer 1600 FT-IR spectrometer. Elemental analyses were performed in the Mikroanalytische Labor of the Technical University Munich (M. Barth). Mass spectra were recorded on a Finnigan MAT 90-spectrometer. Catalytic runs were monitored by chiral GC methods on a Hewlett–Packard (HP 5970 B) instrument equipped with a Chiraldex γ-TA column (Alltech), a mass-selective detector (HP5970 B) and integration unit (HP 3394).

$WO_2(acac)_2$ was prepared according to the procedure from the literature [3]. $MoO_2(acac)_2$, (+)-camphor, (−)-camphor, (−)-fenchone, (−)-menthone, 2-bromopyridine, *tert*-butylhydroperoxide, *trans*-β-methyl styrene, were purchased from Aldrich or Fluka and used without further purification.

4.2. X-ray crystallography

Suitable single crystals for the X-ray diffraction studies were grown by standard techniques from saturated solutions in $CH_3OH/CHCl_3$ at room temperature (r.t.). All structures were solved by a combination of direct methods, difference-Fourier syntheses and least-squares methods. Neutral atom scattering factors for all atoms and anomalous dispersion corrections for the non-hydrogen atoms were taken from the International Tables for X-Ray Crystallography. All calculations were performed on a DEC 3000 AXP workstation with the STRUX-V system, including the programs PLATON-92, SIR-92 AND SHELXL-93 [19].

4.3. Data collection, structure solution and refinement for the complexes **6**, **13** and **19**

A summary of the collection and refinement data are reported in Table 2. Preliminary examination and data collection were carried out in the case of **13** and **19** on an imaging plate diffraction system (IPDS; Stoe & Cie) equipped with a rotating anode (Nonius FR591; 50 kV; 60 mA; 3.0 kW; graphite monochromated Mo–K_α radiation) and in the case of **6** on a four cycle diffractometer (CAD4; Nonius) equipped with a fine focus sealed tube (50 kV; 24 mA; 1.2 kW; graphite monochromated Cu–K_α radiation). The data collection was performed at 193 K within the θ-range of $3.8° < \theta < 67.8°$ (**6**), $2.8° < \theta < 24.6°$ (**13**) and $4.1° < \theta < 26.4°$ (**19**). A total number of 4739 (17 015 and 5854) reflec-

tions were collected. After merging a sum of 4535, 4520 and 5854 independent reflections remained and were used for all calculations. Data were corrected for Lorentz and polarization effects. All 'heavy atoms' of the asymmetric unit were anisotropically refined. The hydrogen atoms were calculated in ideal positions (riding model) for **13** and **19**, for **6** all hydrogen atoms were located in difference Fourier maps and refined isotropically. Full matrix least-squares refinements were carried out by minimizing $Sw(F_o^2-F_c^2)^2$ with the SHELXL weighting scheme and stopped at shift/err < 0.001. The final refinement (on F_o^2) of 475 (362, 530) parameters converged at $R_1 = 0.0535$ (0.0286, 0.0157), $wR_2 = 0.1135$ (0.0477, 0.0416) and GoF = 1.085 (0.916, 1.06).

4.4. General procedure for the synthesis of the ligands 4–7

To a solution of 200 ml dry diethylether under nitrogen was added 80 ml of 1.6 M *n*-butyllithium/hexane at −78°C (dry ice/isopropanol). After 10 min, 11.5 ml (0.123 mmol) of 2-brompyridine dissolved in 10 ml of diethylether was added and the clear solution turned to dark red. The solution was stirred for additional 30 min. After the addition of 130 mmol of the appropriate ketone dissolved in 25 ml of diethylether the reaction solution was stirred for 2 h and the temperature was not allowed to raise above −40°C. The solution was allowed to warm up to r.t. and carefully hydrolyzed by addition of 5 ml of saturated aqueous ammonium chloride solution. For the isolation of the reaction product the organic phase was extracted with 5×100 ml of HCl (10%) solution until the ether phase became almost clear. The aqueous phase was then neutralized with a NaOH (10%) solution until an intense white precipitate occurs followed by extraction with ether. Finally, the organic phase was dried over sodium sulfate, filtered and the solvent removed under high vacuum resulting in a brown residue. The crude product can be further purified by dissolving the product in a small amount of ether, filtration over celite followed by recrystallisation. In all four cases the product was obtained as a colorless crystalline material of analytical purity.

4.4.1. (1R,2R,4R)-1,7,7-Trimethyl-2-(2′-pyridinyl)-bicyclo[2.2.1]heptan-2-ol (4)

Yield: 10.2 g, 36%.

EI-MS: 231 (M^+), 213 (M^+-H_2O). IR (KBr, cm^{-1}): ν(OH) = 3371. ^{1}H-NMR ($CDCl_3$, 400 MHz, 298 K, ppm): $\delta = 8.52$ ($H^{6'}$, d, 1H), 7.63 ($H^{4'}$, dd, 1H), 7.41 ($H^{3'}$, d, 1H), 7.13 ($H^{5'}$, t, 1H), 5.25 (OH, s, 1H), 2.29 (H^{3eq}, m, 1H), 2.08 (H^{3ax}, d, 1H), 1.88 (H^4, t, 1H), 1.78 (H^{5eq}, m, 1H), 1.31 (H^{5ax}, m, 1H), 1.28 (H^{6eq}, m, 1H), 1.25 (H^{10}, s, 3H), 0.81 (H^8, s, 3H), 0.74 (H^{6ax}, m, 1H), 0.71 (H^9, s, 3H). ^{13}C-NMR ($CDCl_3$, 100 MHz, 298 K, ppm): $\delta = 162.3$ ($C^{2'}$, s), 147.37 ($C^{6'}$, d), 135.53 ($C^{4'}$, d), 121.57 ($C^{3'}$, d), 120.58 ($C^{5'}$, d), 82.64 (C^2, s), 53.47 (C^1, s), 50.51 (C^7, s), 45.34 (C^4, d), 44.24 (C^3, t), 30.70 (C^6, t), 26.98 (C^5, t), 21.32 (C^8, q), 21.17 (C^9, q), 9.94 (C^{10}, q).

4.4.2. (1S,2S,4S)-1,7,7-Trimethyl-2-(2′-pyridinyl)-bicyclo[2.2.1]heptan-2-ol (5)

Yield: 10.0 g, 36%.

EI-MS: 231 (M^+), 213 (M^+-H_2O). IR (KBr, cm^{-1}): ν(OH) = 3370. ^{1}H-NMR ($CDCl_3$, 400 MHz, 298 K, ppm): $\delta = 8.52$ ($H^{6'}$, d, 1H), 7.63 ($H^{4'}$, dd, 1H), 7.41 ($H^{3'}$, d, 1H), 7.14 ($H^{5'}$, t, 1H), 5.25 (OH, s, 1H), 2.30 (H^{3eq}, m, 1H), 2.09 (H^{3ax}, d, 1H), 1.88 (H^4, t, 1H), 1.78 (H^{5eq}, m, 1H), 1.31 (H^{5ax}, m, 1H), 1.28 (H^{6eq}, m, 1H), 1.24 (H^{10}, s, 3H), 0.88 (H^8, s, 3H), 0.81 (H^{6ax}, m, 1H), 0.78 (H^9, s, 3H). ^{13}C-NMR ($CDCl_3$, 100 MHz, 298 K, ppm): $\delta = 163.54$ ($C^{2'}$, s), 147.38 ($C^{6'}$, d), 135.55 ($C^{4'}$, d), 121.59 ($C^{3'}$, d), 120.59 ($C^{5'}$, d), 82.65 (C^2, s), 53.48 (C^1, s), 50.51 (C^7, s), 45.36 (C^4, d), 44.24 (C^3, t), 30.71 (C^6, t), 26.99 (C^5, t), 21.33 (C^8, q), 21.17 (C^9, q), 9.94 (C^{10}, q).

4.4.3. (1R,2S,4R)-1,3,3-trimethyl-2-(2′-pyridinyl)-bicyclo[2.2.1]heptan-2-ol (6)

Yield:15.9 g, 56%.

EI-MS (*m*/*z*): 231 (M^+), 213 (M^+-H_2O). IR (KBr, cm^{-1}): ν(OH) = 3364. ^{1}H-NMR ($CDCl_3$, 400 MHz, 298 K, ppm): $\delta = 8.47$ ($H^{6'}$, d, 1H), 7.62 ($H^{4'}$, dd, 1H), 7.51 ($H^{3'}$, d, 1H), 7.12 ($H^{5'}$, t, 1H), 5.82 (OH, s, 1H), 2.32 (H^{6en}, m, 1H), 2.22 (H^7, m, $^3J(H^7, H^7) = 11$ Hz, $^5J(H^7, H^{5en}) = 2$ Hz, $^5J(H^7, H^{6en}) = 1$ Hz), 1.84 (H^{5en}, d, 1H), 1.77 (H^4, d, 1H), 1.47 (H^{5ex}, m, 1H), 1.32 (H^7, d, 1H), 1.12 (H^{6ex}, m, 1H), 0.97 ($H^{8/9}$, s, 3H), 0.95 (H^{10}, s, 3H), 0.41 ($H^{8/9}$, s, 3H). ^{13}C-NMR ($CDCl_3$, 100 MHz, 298 K, ppm): $\delta = 163.25$ ($C^{2'}$, s), 146.69 ($C^{6'}$, d), 134.99 ($C^{4'}$, d), 123.11 ($C^{3'}$, d), 121.35 ($C^{5'}$, d), 83.62 (C^2, s), 51.86 (C^1, s), 48.87 (C^4, d), 45.97 (C^3, s), 42.00 (C^7, t), 32.52 (C^6, t), 29.20 ($C^{9/8}$, q), 24.37 (C^5, t), 22.24 ($C^{9/8}$, q), 17.12 (C^{10}, q).

4.4.4. (1S,2S,5R)-5-Methyl-2-isopropyl-1-(2′-pyridinyl)cyclohexan-1-ol (7)

Yield: 20.6 g, 72%.

EI-MS (*m*/*z*) 233 (M^+); 215 (M^+-H_2O). IR (KBr, cm^{-1}): ν(OH) = 3323. ^{1}H-NMR ($CDCl_3$, 400 MHz, 298 K, ppm): $\delta = 8.48$ ($H^{6'}$, d, 1H), 7.66 ($H^{4'}$, dd, 1H), 7.31 (H^3, d, 1H), 7.14 ($H^{5'}$, t, 1H), 5.20 (OH, s, 1H), 1.95 (H^5, m, 1H), 1.85 (H^{4eq}, m, 1H), 1.70 (H^{3ax}, d, 1H), 1.65 (H^2, m, 1H), 1.58 (H^{3eq}, d, 1H), 1.55 (H^{6eq}, m, 1H), 1.32 (H^{6ax}, dd, 1H), 1.15 (H^7, m, 1H), 1.02 (H^{4ax}, 1H), 0.89 (H^{10}, d, 3H), 0.83 (H^8, d, 3H), 0.67 (H^9, d, 3H). ^{13}C-NMR ($CDCl_3$, 100 MHz, 298 K, ppm): $\delta = 165.35$ ($C^{2'}$, s), 146.97 ($C^{6'}$, d), 136.80 ($C^{4'}$, d), 121.53 ($C^{3'}$, d),

119.25 ($C^{5'}$, d), 77.17 (C^1, s), 50.68 (C^6, t), 50.01 (C^2, d), 35.24 (C^4, t), 28.47 (C^5, d), 27.40 (C^{10}, q), 23.59 (C^5, t), 22.37 (C^8, q), 21.93 (C^3, t), 18.49 (C^9, q).

4.5. General procedures for the synthesis of the dioxomolybdenum(VI) and dioxotungsten(VI) complexes **13–20**

(a) To a solution of 4.3 mmol (2.2 equivalents) of ligands **4–7** in 10 ml of dry methanol under nitrogen atmosphere at r.t. were added 654 mg (2 mmol) (one equivalent) dioxomolybdenum(VI)bis(acetylacetonate) and the resulting suspension was stirred for 30 min. After the reaction has been completed, the volume of the solution was reduced and the reaction products **13–20** precipitate as white microcrystalline solids. The supernatant was filtered off with a Whatman filter-wrapped cannula and the obtained solid washed with cold dry methanol. Finally, the product was dried under high vacuum to give a white powder of analytic purity (^{1}H-NMR). No attempt was made to optimize the product yield. For X-ray diffraction studies the compounds **13** and **19** were recrystallized from methanol/chloroform to give colorless crystals.

(b) An acetic acid solution of 3.6 mmol of ligands **4–7** is added to 75 ml of an aqueous solution of an excess of metal salt, $Na_2[MoO_4]$ or $Na_2[WO_4]$ (10 mmol). The solution is adjusted to pH 4 by adding hydrochloric acid or ammonia. After stirring overnight at r.t. the product is filtered off, washed with hot distilled water and dried in vacuo [20].

4.5.1. Bis[(1R,2R,4R)-1,7,7-trimethyl-2-(2′-pyridinyl)bicyclo[2.2.1]heptan-2-olato]dioxomolybdenum(VI) (**13**)

Yield: 918 mg, 79%.

Anal. Calc. for $C_{30}H_{40}N_2O_4Mo$: C, 59.68; H, 6.78; N, 4.48. Found: C, 59.78; H, 7.13; N, 4.50%. IR (KBr, cm^{-1}): ν(Mo=O) = 902, 912. ^{1}H-NMR ($CDCl_3$, 400 MHz, 298 K, ppm): $\delta = 8.49$ ($H^{6'}$, d, 1H), 7.50 ($H^{4'}$, dd, 1H), 7.11 ($H^{3'}$, d, 1H), 6.97 ($H^{5'}$, t, 1H), 2.70 (H^{3eq}, m, 1H), 1.92 (H^4, dd, 1H), 1.83 (H^{3ax}, d, 1H), 1.80 (H^{5eq}, m, 1H), 1.41 (H^{10}, s, 3H), 1.31 (H^{5ax}, m, 1H), 1.28 (H^{6eq}, m, 1H), 1.22 (H^{6ax}, m, 1H), 0.90 (H^8, s, 3H), 0.83 (H^9, s, 3H). ^{13}C-NMR ($CDCl_3$, 100 MHz, 298 K, ppm): $\delta = 166.07$ ($C^{2'}$, s), 147.74 ($C^{6'}$, d), 137.09 ($C^{4'}$, d), 122.29 ($C^{3'}$, d), 122.20 ($C^{5'}$, d), 96.41 (C^2, s), 51.18 (C^7, s), 50.27 (C^3, t), 45.74 (C^4, d), 31.03 (C^6, t), 27.15 (C^5, t), 21.37 (C^8, q), 20.89 (C^9, q), 11.61 (C^{10}, q).

4.5.2. Bis[(1S,2S,4S)-1,7,7-trimethyl-2-(2′-pyridinyl)bicyclo[2.2.1]heptan-2-olato]dioxomolybdenum(VI) (**14**)

Yield: 953 mg, 82%.

Anal. Calc. for $C_{30}H_{40}N_2O_4Mo$: C, 59.68; H, 6.78; N, 4.48. Found: C, 59.74; H, 7.0214; N, 4.50%. IR (KBr, cm^{-1}): ν(Mo=O) = 902, 912. ^{1}H-NMR ($CDCl_3$, 400 MHz, 298 K, ppm): $\delta = 8.57$ ($H^{6'}$, d, $^3J(H^{6'}, H^{5'}) = 5.2$ Hz, 1H), 7.41 ($H^{4'}$, dd, $^3J(H^{4'}, H^{5'}) = 7.5$ Hz, $^3J(H^{4'}, H^{3'}) = 8.2$ Hz, 1H), 7.15 ($H^{3''}$, d, $^3J(H^{3'}, H^{4'}) = 8.2$ Hz, 1H), 6.99 ($H^{5'}$, dd, $^3J(H^{5'}, H^{6'}) = 6.0$ Hz, $^3J(H^{5'}, H^{4'}) =$ 6.7 Hz, 1H), 2.78 (H^{3eq}, m, 1H), 1.96 (H^4, m, 1H), 1.88 (H^{3ax}, m, 1H), 1.84 (H^{5eq}, m, 1H), 1.47 (H^{10}, s, 3H), 1.32 (H^{5ax}, m, 1H), 1.29 (H^{6eq}, m, 1H), 1.23 (H^{6ax}, m, 1H), 0.93 (H^8, s, 3H), 0.91 (H^9, s, 3H). ^{13}C-NMR ($CDCl_3$, 100 Hz, 298 K, ppm): $\delta = 166.44$ ($C^{2'}$), 147.90 ($C^{6'}$), 136.90 ($C^{4'}$), 122.31 ($C^{3'}$), 121.87 ($C^{5'}$), 96.14 (C^2), 51.36 (C^7), 50.55 (C^3), 45.90 (C^4), 31.19 (C^6), 27.38 (C^5), 21.62 (C^8), 21.06 (C^9), 11.78 (C^{10}).

4.5.3. Bis[(1R,2S,4R)-1,3,3-trimethyl-2-(2′-pyridinyl)bicyclo[2.2.1]heptan-2-olato]dioxomolybdenum(VI) (**15**)

Yield: 929 mg, 80%.

Anal. Calc. for $C_{30}H_{40}N_2O_4Mo$: C, 59.68; H, 6.78; N, 4.48. Found: C, 60.74; H, 6.85; N, 4.63%. IR (KBr, cm^{-1}): ν(Mo=O) = 921, 896. ^{1}H-NMR ($CDCl_3$, 400 MHz, 298 K, ppm): $\delta = 8.82$ ($H^{6'}$, d, 1H), 7.69 ($H^{4'}$, dd, 1H), 7.61 ($H^{3'}$, d, 1H), 7.17 ($H^{5'}$, t, 1H), 3.40 (H^{3eq}, m, 1H), 1.83 (H^{3ax}, d, 1H), 1.92 (H^4, dd, 1H), 1.80 (H^{5eq}, m, 1H), 1.41 (H^{10}, s, 3H), 1.31 (H^{5ax}, m, 1H), 1.28 (H^{6eq}, m, 1H), 1.20 (H^{6ax}, m, 1H), 0.79 (H^8, s, 3H), 0.69 (H^9, s, 3H). ^{13}C-NMR ($CDCl_3$, 100 MHz, 298 K, ppm): $\delta = 164.94$ ($C^{2'}$), 147.15 ($C^{6'}$), 136.66 ($C^{4'}$), 124.36 ($C^{3'}$), 121.91 ($C^{5'}$), 99.62 (C^2), 54.74 (C^1), 50.65 (C^4), 49.08 (C^3) 42.78 (C^7), 31.81 (C^6), 30.12 (C^8), 24.94 (C^5), 22.21 (C^9), 18.88 (C^{10}).

4.5.4. Bis[(1S,2S,5R)-5-methyl-2-isopropyl-1-(2′-pyridinyl)cyclohexan-1-olato]diooxomolybdenum(VI) (**16**)

Yield: 974 mg, 84%.

Anal. Calc. for $C_{30}H_{44}N_2O_4Mo$: C, 59.80; H, 7.48; N, 4.73. Found: C, 59.78; H, 7.98; N, 4.27%. IR (KBr, cm^{-1}): ν(Mo=O) 916, 902 cm^{-1}. ^{1}H-NMR ($CDCl_3$, 400 MHz, 298 K, ppm): $\delta = 8.79$ ($H^{6'}$, d, 1H), 7.77 ($H^{4'}$, dd, 1H), 7.29 ($H^{3'}$, d, 1H), 7.24 ($H^{5'}$, t, 1H), 2.28 (H^5, m, 1H), 1.95 ($H^{3,4}$, m, 2H), 1.68 ($H^{2,4,6}$, m), 1.65 (H^2, m, 1H), 1.50 (H^7, m, 1H), 1.32 (H^6, d, 1H), 1.04 (H^3, m, 1H), 0.99 (H^{10}, d, 3H), 0.83 ($H^{8,9}$, d, 3H), 0.57 ($H^{8,9}$, d, 3H). ^{13}C-NMR ($CDCl_3$, 100 MHz, 298 K, ppm): $\delta =$ 169.65 ($C^{2'}$, s), 147.70 ($C^{6'}$, d), 136.74 ($C^{4'}$, d), 122.31 ($C^{3'}$, d), 120.35 ($C^{5'}$, d), 92.81 (C^1, s), 54.09 (C^2, t), 50.34 (C^6, t), 35.24 (C^3, t), 28.54 (C^5, d), 27.06 (C^7, d), 24.48 (C^{10}, q), 22.48 (C^4, t), 21.98 ($C^{8/9}$, q), 19.83 ($C^{9/8}$, q).

4.5.5. Bis[(1R,2R,4R)-1,7,7-trimethyl-2-(2′-pyridinyl)bicyclo[2.2.1]heptan-2-olato]dioxotungsten(VI) (**17**)

Yield: 408 g, 83%.

Anal. Calc. for $C_{30}H_{40}N_2O_4W \cdot H_2O$: C, 51.88; H, 6.10; N, 4.03. Found: C, 51.97; H, 6.12; N, 3.82%. MS

(CI, 70 eV) m/z (%) = 678.5 (0.77) [$M^+ + 2$], 676.5 (1.03) [M^+], 247.3 (2.89), 231.2 (22.11), 121.0 (100). IR (KBr, cm^{-1}) ν = 929s [ν_{as}(W=O)], 898s [ν_s(W=O)]. ^{1}H-NMR ($CDCl_3$, 400 MHz, 298 K, ppm): δ = 8.64 ($H^{6'}$, d, $^3J(H^{6'}, H^{5'})$ = 4.5 Hz, 1H), 7.59 ($H^{4'}$, dd, $^3J(H^{4'}, H^{3'})$ = 9 Hz, $^3J(H^{4'}, H^{5'})$ = 7 Hz, 1H), 7.20 ($H^{3'}$, d, $^3J(H^{3'}, H^{4'})$ = 6.5 Hz, 1H), 7.05 ($H^{5'}$, t, $^3J(H^{5'}, H^{6'})$ = 8 Hz, $^3J(H^{5'}, H^{4'})$ = 7 Hz, 1H), 2.82 (H^{3eq}, dt, $^3J(H^{3ex}, H^{3en})$ = 13 Hz, 1H), 1.99 (H^4, dd, $^3J(H^4, H^{3ex})$ = 4 Hz, 1H), 1.88 (H^{5ex}, m, 1H), 1.84 (H^{3ax}, d, $^3J(H^{3en}, H^{3ex})$ = 13 Hz, 1H), 1.51 (H^{10}, s, 3H), 1.38 (H^{5en}, m, 1H), 1.22 (H^{6ex}, m, 1H), 1.20 (H^{6en}, m, 1H), 0.99 (H^8, s, 3H), 0.94 (H^9, s, 3H). ^{13}C-NMR ($CDCl_3$, 100 MHz, 298 K, ppm): δ = 166.06 ($C^{2'}$), 146.92 ($C^{6'}$), 136.37 ($C^{4'}$), 121.74 ($C^{3'}$), 121,20 ($C^{5'}$), 94.81 (C^2), 59.42 (C^1), 50.48 (C^7), 49.82 (C^3), 44.95 (C^4), 30.07 (C^6), 26.38 (C^5), 20.55 (C^8), 20.07 (C^9), 10.85 (C^{10}).

4.5.6. Bis[(1S,2S,4S)-1,7,7-trimethyl-2-(2′-pyridinyl)-bicyclo[2.2.1]heptan-2-olato]dioxotungsten(VI) ***(18)***

Yield: 399 g, 81%.

Anal. Calc. for $C_{30}H_{40}N_2O_4W{\cdot}H_2O$: C, 51.88; H, 6.10; N, 4.03. Found: C, 51.93; H, 6.14; N, 3.91%. MS (CI, 70 eV) m/z (%) = 678.5 (0.77) [$M^+ + 2$], 676.5 (1.03) [M^+], 247.3 (2.89), 231.2 (22.11), 121.0 (100). IR (KBr, cm^{-1}) ν = 929s [ν_{as}(W=O)], 898s [ν_s(W=O)]. ^{1}H-NMR ($CDCl_3$, 400 MHz, 298 K, ppm): δ = 8.64 ($H^{6'}$, d, $^3J(H^{6'}, H^{5'})$ = 5.2 Hz, 1H), 7.59 ($H^{4'}$, dd, $^3J(H^{4'}, H^{3'})$ = 7.5 Hz, $^3J(H^{4'}, H^{5'})$ = 7.5 Hz, 1H), 7.19 ($H^{3'}$, d, $^3J(H^{3'}, H^{4'})$ = 7.5 Hz, 1H), 7.05 ($H^{5'}$, t, $^3J(H^{5'}, H^{6'})$ = 6.8 Hz, $^3J(H^{5'}, H^{4'})$ = 6.0 Hz, 1H), 2.82 (H^{3eq}, dt, $^3J(H^{3ex}, H^{3en})$ = 13.5 Hz, 1H), 1.99 (H^4, m, 1H), 1.86 (H^{5ex}, m, 1H), 1.83 (H^{3ax}, m, 1H), 1.56 (H^{10}, s, 3H), 1.38 (H^{5en}, m, 1H), 1.26 (H^{6ex}, m, 1H), 1.23 (H^{6en}, m, 1H), 0.99 (H^8, s, 3H), 0.93 (H^9, s, 3H). ^{13}C-NMR ($CDCl_3$, 100 MHz, 298 K, ppm): δ = 167.06 ($C^{2'}$), 147.92 ($C^{6'}$), 137.36 ($C^{4'}$), 122.74 ($C^{3'}$), 122,21 ($C^{5'}$), 95.83 (C^2), 60.44 (C^1), 51.48 (C^7), 50.82 (C^3), 45.91 (C^4), 31.07 (C^6), 27.38 (C^5), 21.55 (C^8), 21.06 (C^9), 11.86 (C^{10}).

4.5.7. Bis[(1R,2S,4R)-1,3,3-trimethyl-2-(2′-pyridinyl)-bicyclo[2.2.1]heptan-2-olato]dioxotungsten(VI) ***(19)***

Yield: 434 g, 88%.

Anal. Calc. for $C_{30}H_{40}N_2O_4W{\cdot}H_2O$: C, 51.88; H, 6.10; N, 4.03. Found: C, 51.77; H, 6.47; N, 3.86%. MS (CI, 70 eV) m/z (%) = 678.8 (95.84) [$M^+ + 2$], 676.8 (100.0) [M^+], 659.8 (16.37), 594.9 (4.41), 230.0 (4.71), 214.0 (70.16), 143.8 (4.14). IR (KBr, cm^{-1}) ν = 932 [ν_{as}(W=O)], 896 [ν_s(W=O)]. ^{1}H-NMR ($CDCl_3$, 400 MHz, 298 K, ppm): δ = 8.87 ($H^{6'}$, d, $^3J(H^{6'}, H^{5'})$ = 5 Hz, 1H), 7.72 ($H^{4'}$, t, $^3J(H^{4'}, H^{3'})$ = 8 Hz, $^3J(H^{4'}, H^{5'})$ = 6 Hz, 1H), 7.65 ($H^{3'}$, d, $^3J(H^{3'}, H^{4'})$ = 8 Hz, 1H), 7.23 ($H^{5'}$, t, $^3J(H^{5'}, H^{4'})$ = 6 Hz, 1H), 2.68 (H^{6en}, m, 1H), 2.24 (H^{7en}, d, $^2J(H^{7en}, H^{7en})$ = 10.5 Hz, 1H), 2.04 (H^{5en}, m, 1H), 1.77 (H^4, m, 1H), 1.55 (H^{5ex}, m, 1H), 1.45 (H^{10}, s, 3H) 1.32 (H^{7ex}, m, 1H), 1.22 (H^{6ex}, m, 1H), 0.80 (H^8, s, 3H), 0.72 (H^9, s, 3H). ^{13}C-NMR ($CDCl_3$, 100 MHz, 298 K, ppm): δ = 165.57 ($C^{2'}$), 147.43 ($C^{6'}$), 137.12 ($C^{4'}$), 124.67 ($C^{3'}$), 122.18 ($C^{5'}$), 99.41(C^2), 55.18 (C^1), 50.20 (C^4), 49.07 (C^3), 42.97 (C^7), 31.73 (C^6), 29.98 (C^8), 25.00 (C^5), 22.40 (C^9), 18.93 (C^{10}).

4.5.8. Bis[(1S,2S,5R)-5-methyl-2-isopropyl-1-(2′-pyridinyl)cyclohexan-1-olato]dioxotungsten(VI) ***(20)***

Yield: 450 g, 91%.

Anal. Calc. for $C_{30}H_{44}N_2O_4W{\cdot}2H_2O$: C, 50.29; H, 6.75; N, 3.91. Found: C, 50.19; H, 6.92; N, 3.57%. MS (CI, 70 eV) m/z (%) = 679.8 (43.61) [M^+], 661.8 (35.89), 594.8 (8.54), 568.7 (2.23), 463.9 (10.93), 354.9 (2.54), 233.0 (10.89), 216.0 (100.00), 148.0 (27.42). IR (KBr, cm^{-1}) ν = 934 [ν_{as}(W=O)], 896 [ν_s(W=O)]. ^{1}H-NMR ($CDCl_3$, 400 MHz, 298 K, ppm): δ = 8.82 ($H^{6'}$, d, $^3J(H^{6'}, H^{5'})$ = 5.1 Hz, 1H), 7.80 ($H^{4'}$, dd, $^3J(H^{4'}, H^{5'})$ = 6 Hz, 1H), 7.33 ($H^{3'}$, d, $^3J(H^{3'}, H^{4'})$ = 6 Hz, 1H), 7.31 ($H^{5'}$, t, $^3J(H^{5'}, H^{4'})$ = 6 Hz, 1H), 3.45 (H^2, d, $^3J(H^2, H^7)$ = 4 Hz, 1H), 2.29 (H^5, m, 1H), 1.95 (H^3, d, 1H), 1.71 (H^6, m, 1H), 1.68 (H^2, m, 1H), 1.65 (H^6, m, 1H), 1.33 (H^6, dd, $^3J(H^{6ax}, H^{6eq})$ = 8 Hz, 1H), 1.10 (H^7, m, 1H), 1.03 (H^{10}, d, $^3J(H^{10}, H^5)$ = 6.9 Hz, 3H), 0.94 (H^8, d, $^3J(H^8, H^7)$ = 6.9 Hz, 3H), 0.59 (H^9, d, $^3J(H^9, H^7)$ = 6.6 Hz, 3H). ^{13}C-NMR ($CDCl_3$, 100 MHz, 298 K, ppm): δ = 170.18 ($C^{2'}$), 147.99 ($C^{6'}$), 139.14 ($C^{4'}$), 122.60 ($C^{3'}$), 120.69 ($C^{5'}$), 92.52 (C^1), 54.06 (C^6), 50.61 (C^2), 35.29 (C^4), 28.53 (C^5), 26.91 (C^{10}), 24.63 (C^5), 22.53 (C^8), 21.96 (C^3), 20.00 (C^9).

4.6. General procedure for the epoxidation of trans-β-methylstyrene with molybdenum and tungsten compounds ***13–20***

A total of 200 mg (1.7 mmol) of *trans*-β-methylstyrene and 10 mg (1.0 mol%) catalyst was dissolved in 2 ml of chloroform. After the addition of 615 μl (5.5 M) of *tert*-butyl hydroperoxide solution, the reaction mixture was stirred for up to 16 h at 50°C.

For GC-analysis aliquots of 10 μl were taken, quenched with manganese dioxide at 0°C on an ice bath, diluted with 1 μl of chloroform and dried over magnesium sulfate. The enantiomeric excess and conversion was determined on a chiral GC column. The products were identified by GC/MS and co-injection of reference substances.

5. Supplementary material

Crystallographic data (excluding structure factors) for the structural analysis have been deposited with the Cambridge Crystallographic Data Centre, CCDC nos. 138893 for **6**, 138894 for **13** and 138895 for **19**. Copies of the data can be obtained free of charge from The

Director, CCDC, 12 Union Rd., Cambridge CB2 1EX, UK (Fax: +44-1223-336033; e-mail: deposit@ccdc.com.ac.uk or www: http://www.ccdc.cam.ac.uk).

Acknowledgements

This work was financially supported by the Deutsche Forschungsgemeinschaft (SPP Sauerstofftransfer/Peroxidchemie) and the Bayerische Forschungsverbund für Katalyse (FORKAT).

References

[1] W.A. Herrmann, G.M. Lobmaier, T. Priermeier, M.R. Mattner, B. Scharbert, J. Mol. Catal. 117 (1997) 455.
[2] (a) W.A. Herrmann, G.M. Lobmaier, U. Dingerdissen, R. Schulz (Hoechst AG), DE-A-197 29 837, 1997. (b) W.A. Herrmann, G.M. Lobmaier, U. Dingerdissen, B. Scharbert, R. Schulz (Hoechst AG), DE-A-197 29 838, 1997.
[3] W.A. Herrmann, J. Fridgen, G.M. Lobmaier, M. Spiegler, New J. Chem. (1999) 5.
[4] (a) S.-I. Yamada, T. Mashiko, S. Terashima, J. Am. Chem. Soc. 99 (1977) 1988. (b) S. Coleman Kammula, E.T. Duim-Kollstra, J. Organomet. Chem. 246 (1983) 53. (c) V. Schurig, K. Hintzer, U. Leyrer, C. Mark, P. Pitchen, H.B. Kagan, J. Organomet. Chem. 370 (1989) 81. (d) H. Brunner, H. Zintl, J. Organomet. Chem. 411 (1991) 375. (e) K. Kaneda, S. Haruna, T. Imanaka, M. Hamamoto, Y. Nishiyama, Y. Ishii, Tetrahedron Lett. 33 (1992) 6827.
[5] (a) B.E. Schultz, S.F. Gheller, M.C. Muetterties, M.J. Scott, R.H. Holm, J. Am. Chem. Soc. 115 (1993) 2714. (b) W.A. Herrmann, G.M. Lobmaier, T. Priermeier, M.R. Mattner, B. Scharbert, J. Mol. Catal. 117 (1997) 455. (c) G.M. Lobmaier, Ph.D. Thesis, Technische Universität München, Munich, 1997. (d) I. Kim, Y. Nishihara, R.F. Jordan, R.D. Rogers, A.D. Rheingold, G.P.A. Yap, Organometallics 16 (1997) 314. (e) J. Fridgen, Diploma Thesis, Technische Universität München, Munich, 1998.
[6] T.J. Collins, Acc. Chem. Res. 27 (1994) 279.
[7] (a) G. Chelucci, F. Soccolini, Tetrahedron Asymmetry 3 (1992) 1235. (b) M. Genov, K. Kostova, V. Dimitrov, Tetrahedron Asymmetry 8 (1997) 1869.
[8] (a) W.A. Herrmann, J.J. Haider, G.M. Lobmaier, The XVIIIth International Conference on Organometallic Chemistry (ICOMC), Munich, Germany, 16–21 August, 1998. (b) W.A. Herrmann, J.J. Haider, J. Fridgen, M. Spiegler, 7th International Symposium on Dioxygen Activation and Homogeneous Catalytic Oxidation (ADHOC-99), York, UK, 19–23 July, 1999. (c) W.A. Herrmann, J. Fridgen, M. Spiegler, Conference on Organometallic Chemistry 1999 (XIIIth FECHEM), Lisbon, Portugal, August 29th–September 3rd, 1999.
[9] J.I. Uenishi, T. Hiraoka, S. Hata, K. Nishiwaki, O. Yoemitsu, J. Org. Chem. 63 (1998) 2481.
[10] C. Bolm, M. Ewald, M. Felder, G. Schlingloff, Chem. Ber. 125 (1992) 1169.
[11] (a) N.T. Ahn, Top. Curr. Chem. 88 (1980) 145. (b) J. Mulzer, Nachr. Chem. Tech. Lab. 32 (1984) 16. (c) M. Cherest, H. Felkin, N. Prudent, Tetrahedron Lett. 1 (1968) 4199.
[12] (a) J.J. Haider, Ph.D. Thesis, Technische Universität München, Munich, 1998. (b) W.A. Herrmann, J.J. Haider, G.M. Lobmaier, R.W. Fischer, DE 19827046 AI.
[13] Unpublished results except for complex 13 and 19.
[14] (a) E.N. Jacobsen, in: I. Ojima (Ed.) Catalytic Asymmetric Syntheses, VCH, Weinheim, 1993, p. 159. (b) E.N. Jacobsen, W. Zhang, A.R. Muci, D.R. Ecker, L. Deng, J. Am. Chem. Soc. 113 (1991) 7063. (c) E.N. Jacobsen, W. Zhang, L. Deng (Research Corporation Technologies, Inc.), WO 93/03838, 1991 [Chem. Abstr. 120 (1994) 7876v].
[15] K. Tani, M. Hanafusa, S. Otsuka, Tetrahedron Lett. (1979) 3017.
[16] (a) C. Venturello, Chim. Ind. 75 (1993) 283. (b) K.A. Jorgensen, Chem. Rev. 89 (1989) 431. (c) M. Quenard, V. Bonmarin, G. Gelbard, L. Krumenacker, New. J. Chem. 13 (1989) 183. (d) O. Bortolini, F.D. Furia, G. Modena, R. Seraglia, J. Org. Chem. 50 (1985) 2688. (e) J. Prandi, H.B. Kagan, H. Mimoun, Tetrahedron Lett. 27 (1986) 2617. (f) S. Sakaguchi, Y. Nishiyama, Y. Ishii, J. Org. Chem. 61 (1996) 5307. (g) C. Venturello, E. Alneri, M. Ricci, J. Org. Chem. 48 (1983) 2831. (h) H.C. Stevens, A.J. Kaman, J. Am. Chem. Soc. 87 (1965) 734. (i) L. Salles, F. Robert, V. Semmer, Y. Jeannin, J.-M. Brégeault, Bull. Soc. Chim. Fr. 133 (1996) 319.
[17] R. Sheldon, in: W.A. Herrmann, B. Cornils (Eds.), Applied Homogeneous Catalysis with Organometallic Compounds, vol. 2, VCH-Wiley, Weinheim, 1996, p. 411.
[18] R.A. Sheldon, Top. Curr. Chem. 164 (1993) 21.
[19] (a) IPDS Operating System Version 2.8, Stoe & Cie, GmbH, Darmstadt, Germany, 1997. (b) A. Altomare, G. Cascarano, C. Giacovazzo, A. Guagliardi, M.C. Burla. (c) G. Polidori, M. Camalli, SIR-92, University Bari, Italy, 1992. (d) A.J.C. Wilson (Ed.) International Tables for Crystallography, vol. C, tables 6.1.1.4 (pp. 500–502, 219–222) and 4.2.4.2 (pp. 193–199), Kluwer Academic Publishers, Dordrecht, The Netherlands, 1992. (e) G.M. Sheldrick, SHELXL-93, in: G.M. Sheldrick, C. Krüger, R. Goddard (Eds.), Crystallographic Computing 3, Oxford University Press, UK, 1993, pp. 175–189. (f) A.L. Spek, PLATON-92, An Integrated Tool for the Analysis of the Results of a Single Crystal Structure Determination, Acta Crystallogr. Sect. A 46 (1990) C34.
[20] T. Honjo, S. Kawasaki, Bull. Chem. Soc. Jpn. 61 (1988) 2247.